

Combined FTIR and Temperature Programmed Fischer-Tropsch Synthesis over Ru/SiO₂ and Ru-Ag/SiO₂ Supported Catalysts

Syed T. Hussain,* M. Arif Nadeem, M. Mazhar, and Faical Larachi†

Department of Chemistry, Quaid-i-Azam University, Islamabad-45320, Pakistan. *E-mail: dr_tajamul@yahoo.ca

†Department of Chemical Engineering, University of Laval, Quebec, Canada, G1K 7P4

Received October 10, 2006

Combined temperature programmed reaction (TPR) and infrared (IR) spectroscopic studies for Fischer-Tropsch reaction have been performed over Ru/SiO₂ and Ru-Ag/SiO₂ supported catalysts. Reaction of linearly absorbed CO with hydrogen starts at 375 K over Ru/SiO₂ catalyst and reaches maximum at 420 K accompanied with an intensity decrease of linear CO absorption. The reaction with bridged absorbed CO peaks around 510-535 K. Addition of Ag yields mixed Ru-Ag bimetallic sites while it suppresses the formation of bridged bonded CO. Formation of methane on this modified surface occurs at 390 K and reaches maximum at 444 K. Suppression of hydrogen on the Ag-doped surface also occurs resulting in the formation of unsaturated hydrocarbons and of CH_x intermediates not observed with Ru/SiO₂ catalyst. Such intermediates are believed to be the building blocks of higher hydrocarbons during the Fischer-Tropsch synthesis. Linearly absorbed CO is found to be more reactive as compared to bridged CO. The Ag-modified surface also produces CO₂ and carbon. On this surface, hydrogenation of CO begins at 390 K and reaches maximum at 494 K. The high temperature for hydrogenation of absorbed CO and C over Ru-Ag/SiO₂ catalyst as compared to Ru/SiO₂ catalyst is due to the formation of Ru-Ag bimetallic surfaces impeding hydrogen adsorption.

Key Words : Ru/silica, Ru-Ag/silica catalyst, Fischer-Tropsch reaction, *In-situ* infrared and TPR-MS characterization

Introduction

Several studies of Fischer-Tropsch synthesis have been conducted on Ru/SiO₂ catalyst because of its unique property for hydrocarbon products.¹⁻³ The mechanism by which CO adsorbs on the catalyst surface is still a matter of investigation and which mode of CO adsorption is more active for hydrogenation to hydrocarbon is still a matter of debate among the catalyst research circle. It has been documented in the literature that different forms of CO could exhibit different reactivities.⁴⁻⁶ Linear CO has been shown to be involved in CO insertion, which controls catalyst activity and selectivity to higher hydrocarbon.⁷ In contrast, bridged CO sites exhibit little CO insertion activity. The blocking of bridged CO sites by Ag^{8,9} causes an increase in unsaturated hydrocarbon selectivity and a decrease in methanation selectivity. Other promoters such as Mn,¹⁰ La,¹¹ Ti¹² and V¹³ also exhibit an increase in higher hydrocarbon selectivity, but these promoters do not exhibit the formation of bridge CO sites over Ru/SiO₂ catalyst.^{14,15}

The reactivity of absorbed CO has been studied using various methods to identify the form of absorbed CO species responsible for methanation. Using a pulse surface reaction rate analysis, Mori *et al.* found linear CO to be responsible for methanation over Rh/Al₂O₃¹⁶ and Ru/Al₂O₃¹⁷ catalysts. In contrast, temperature programmed reaction (TPR) and separate IR spectroscopic studies conducted by Fujimoto *et al.*¹⁸ have suggested bridged CO to be the active species for methanation over Rh/Al₂O₃ catalyst. Solymosi and coworkers¹⁹ using a flow technique and IR spectroscopic studies on

supported Rh have suggested that the dissociation of linear CO occurs through the formation of Rh-carbonyl-hydride species. Although the linear CO was found to be more stable than the bridged CO on Ru(III) single crystal and less stable on Ni(III) single crystal, the site for CO dissociation on metal surfaces is still unclear.^{20,21}

The objective of this work is to study the reactivity of linear and bridged CO towards hydrogenation for methanation and higher hydrocarbons as well as the effect of Ag on methanation sites of supported Ru catalysts. CO adsorption/reaction on Ru/SiO₂ and Ag-Ru/SiO₂ catalysts has been studied using an in-situ IR spectroscopy technique coupled with temperature programmed reaction (TPR). The intensity decrease of linear and bridged CO with increasing methane formation was monitored to identify their roles in methanation and formation of higher hydrocarbons. TPR allows the study of the catalyzed reaction and yields kinetics data and insight into the reaction mechanism, which is not obtained through steady-state experiments.²²

Experimental

Catalyst Preparation. A 1% w/w Ru/SiO₂ catalyst was prepared by impregnation of large pore size silica (300 m²g⁻¹) using ruthenium chloride solution. The ratio of the solution volume to the material's support weight used is 1 cm³/g. Supported Ag-Ru/SiO₂ catalyst (with Ag to Ru molar ratio 1:1, 0.2% Ag and 1% Ru w/w) was prepared by co-impregnation of ruthenium chloride and silver nitrate solutions. After impregnation, both catalysts were dried

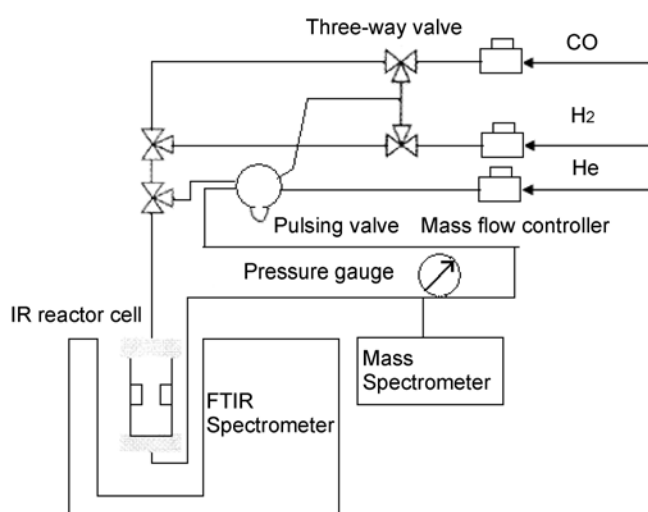


Figure 1. Schematic diagram of the experimental apparatus for combined IR and TPR studies.

overnight in air at 320 K. They were then reduced in flowing hydrogen at 673 K for 16 hours and 30 cm³/min H₂ volumetric flow rate.

The catalyst samples were characterized by BET surface area and CO chemisorption. The catalyst samples were pressed into self-supporting disks and then placed in an IR cell (Bio-Rad FTS 6000 spectrometer). The samples were reduced in-situ at 673K before TPR studies.

TPR Studies. A layout of the temperature programmed reaction apparatus used in the study is presented in Figure 1. The IR cell, made up of Hastelloy, is capable of operating up to 760 K and 8.0 MPa. CO was introduced into the IR cell to adsorb on the surface of the catalyst at 298 K and 0.15 MPa. The gas phase CO was removed by flowing helium through the reactor. The TPR was performed at 20 cm³/min helium flow (10% H₂ in He) at a ramping rate of 15 K/min from 298 to 670 K. At this temperature the flow was held for 15 min. An IR spectrum was recorded by an FTIR spectrometer with DTGS detector at 6 cm⁻¹ resolution. The gaseous effluent from the IR cell was monitored by Balzer QMG 511 mass spectrometer. The spectrum shows the presence of methane (m/e = 16), CO (m/e = 28), CO₂ (m/e = 44) and H₂O (m/e = 18). On Ag doped samples, C₂H₄ and C₂H₆ products were also detected but not in significant quantity.

Results and Discussion

Table 1 & 2 presents the BET surface area, CO-chemisorption, %age dispersion and the products amount formed on Ru/SiO₂ and Ru-Ag/SiO₂ catalyst system.

Figure 2 shows the IR spectra of CO adsorbed on the Ru/SiO₂ catalyst during TPR with hydrogen. The IR spectra for CO absorption at 298 K and 0.15 MPa of CO in a flow of helium through the reactor show a linear band at 2058 cm⁻¹ and a bridged band at 1870 cm⁻¹. A switch from pure He to a flow of H₂/He mixture and an increase in reaction temperature caused a decrease in the intensity of both linear and bridged CO. The rate of decrease in intensity varied with

Table 1. BET surface area, CO uptake, crystallite size of Ru/SiO₂ and Ru-Ag/SiO₂ catalysts

Sample	BET (m ² g ⁻¹)	CO uptake (cm ³ /g)	%age Metal Dispersion
Ru/SiO ₂	125	0.32	24.5
Ag-Ru/SiO ₂	136	0.41	31.2

Table 2. Products' amount formed during TPR over Ru/SiO₂ and Ag-Ru/SiO₂ catalysts

Catalyst	Ru/SiO ₂		Ru-Ag/SiO ₂	
	Peak temperature (K)	Product amount (μmol/g cat.)	Peak temperature (K)	Product amount (μmol/g cat.)
CO	366	15.1	328	13.7
CO ₂	339	2.1	317	10.0
CH ₄	420	16.9	442	7.8
C ₂ H ₄ /C ₂ H ₆	–	–	453	1.0/0.2

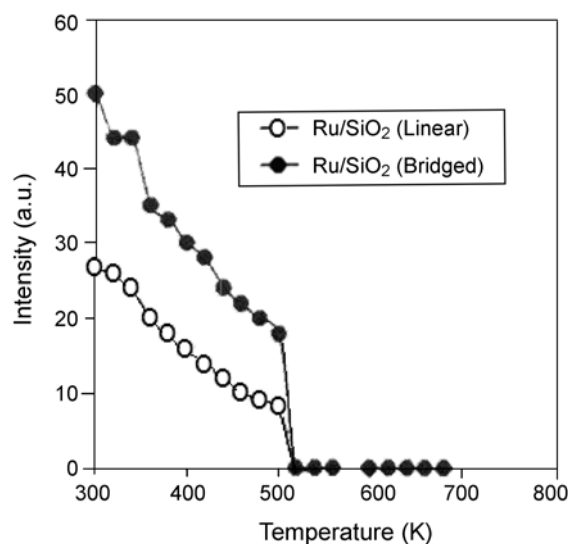


Figure 2. Infrared spectra of temperature-programmed reaction between adsorbed CO and H₂ on Ru/SiO₂ catalyst.

temperature.

The major gas phase products resulting from TPR include CO, CH₄, H₂O and CO₂ whose TPR profiles are shown in Figure 3. The gas phase CO profile from the IR cell effluent exhibits desorption peak at about 366 K while the CO₂ profile exhibited a weak band from 317 to 426 K. In the same temperature range, the linear CO intensity decreased more rapidly than the bridged CO intensity did. The majority of gaseous CO may be produced from the linearly adsorbed CO providing that rapid exchange between linear CO and bridged CO did not occur during TPR. The slight decrease in the bridge CO peak indicates that this latter species is more stable in this temperature range than linear CO.

The rapid decrease in linear CO intensity corresponding to the methane peak at 420 K indicates that the linear CO is more reactive towards H₂ than bridge CO leading to methane formation. A conspicuous contribution of the bridged CO

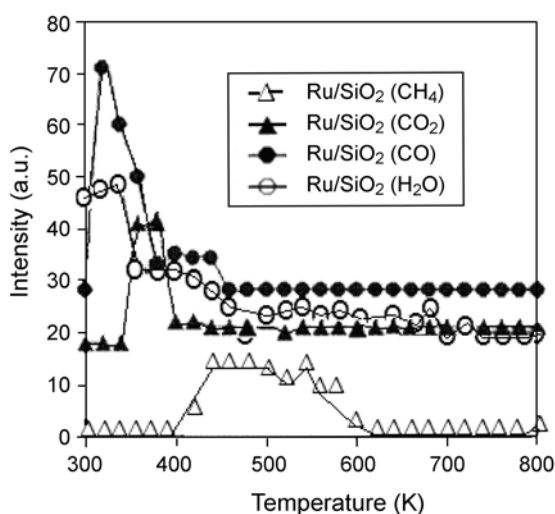


Figure 3. Products response distribution from TPR-MS profile as a function of temperature:

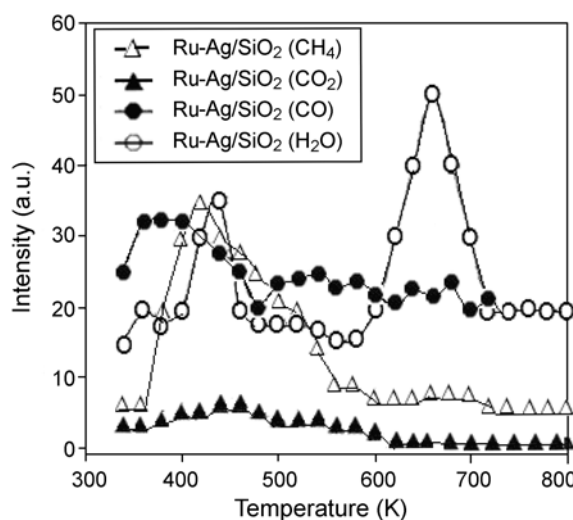


Figure 5. Products response distribution from TPR-MS profile as a function of temperature: Ru-Ag/SiO₂ catalyst.

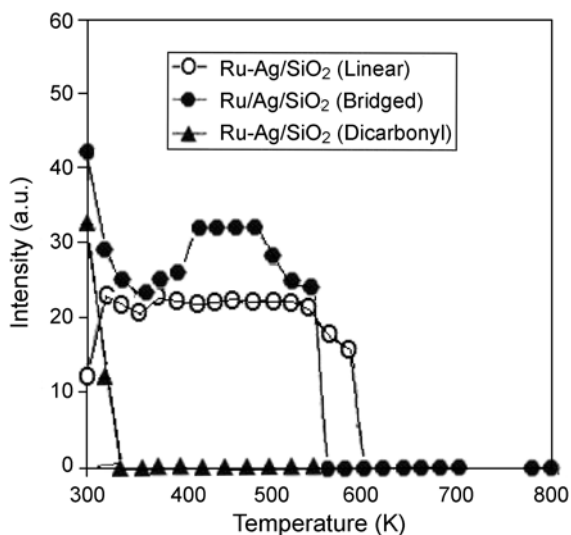


Figure 4. Infrared spectra of temperature-programmed reaction between adsorbed CO and H₂ on Ru-Ag/SiO₂ catalyst

was observed at 510–535 K where a rapid decrease in both bridged and linear CO intensities and the appearance of a tailing methane shoulder occurred. The oxygen generated from the dissociation of CO combined primarily with hydrogen to yield water and the reaction of this oxygen with the undissociated CO did not occur to a significant extent. The formation of water occurred at higher temperature than the hydrogenation of surface carbon to methane did.

The IR spectra of CO adsorbed on Ag-Ru/SiO₂ catalyst during TPR are shown in Figure 4. The IR spectra of adsorbed CO at 298 K and 0.15 MPa of CO in a flow of He through the reactor show a linear CO band at 2000 cm⁻¹, a weakly bridged band around 1870 cm⁻¹, a symmetric vibration of gem-dicarbonyl band at 2093 cm⁻¹ and vague shoulder at 2036 cm⁻¹ due to asymmetric vibration of gem-dicarbonyl. The formation of gem-dicarbonyl suggests the presence of isolated Ru sites on Ag-Ru/SiO₂. Switching from He flow to

a mixture of H₂ and He led to slight increase in the ratio of bridged to linear CO.

Increasing the temperature caused an initial decrease and then a slight increase in the linear CO intensity. An initial increase in the intensity of bridged CO band and a decrease in the intensity of the gem-dicarbonyl band are also observed with an increase in temperature. The growth of the bridged CO band at the expense of gem-dicarbonyl band in hydrogen flow suggests the occurrence of reductive agglomeration of Ru⁺ leading to the formation of Ru crystallite. Increase in the bridged CO intensity and decrease in the linear CO intensity at low temperature also suggests that (i) linear CO may be involved in CO desorption and CO₂ formation at temperature below 360 K and (ii) aggregation of Ag atoms at the expense of inter-dispersed Ag atoms on ruthenium crystallites. The aggregation of Ag atoms on Ru surface due to reactant induced surface reconstruction has been observed under CO hydrogenation conditions (which results in a decrease in the intensity ratio of linear to bridged CO).

The major gas phase products resulting from TPR include CO, CH₄ and CO₂ whose TPR profiles are shown in Figure 5. Both gaseous CO and CO₂ peaks were observed in the temperature range 310–375 K where linear CO and gem-dicarbonyl band show rapid decline in intensity. Bridged CO appears to play little role in CO₂ formation in this temperature range. Contribution of linear CO on Ru-Ag/SiO₂ towards CO₂ should not be significant as indicated by the formation of small quantity of CO₂ from linear CO on Ru/SiO₂. The formation of the CO₂ peak could either be due to (i) disproportionation of gem-dicarbonyl CO or (ii) reduction of Ru⁺ through oxidation of CO ligand of a Ru⁺(CO)₂ [2Ru⁺(CO)₂ + O²⁻ → Ru(CO) + CO₂ + 2CO], where O²⁻ is a surface oxide oxygen. The occurrence of the latter reaction would lead to the simultaneous formation of CO and CO₂. The slight difference in peak temperature exhibited by CO and CO₂ suggests that the reduction of Ru⁺ through oxidation

of CO ligand of $\text{Ru}^+(\text{CO})_2$ may occur to some extent. Such a reduction process can result in the formation of reduced Ru that chemisorb both linear and bridged CO. The area under the CO peak at 328 K corresponds to 12.8 μmol of CO; the area under the CO_2 peak at 317 K corresponds to 10.0 μmol of CO_2 . The ratio of formation of CO to CO_2 in the temperature range 310-375 K does not fall in the expected 2:1 stoichiometric ratio, which suggests that part of the CO_2 probably resulted from the disproportionation of gem-dicarbonyl. CO disproportionation has also been found to be the major pathway for CO_2 from $\text{Ru}^+(\text{CO})_2$ on $\text{RuCl}_3/\text{SiO}_2$.

The disproportionation reaction is accompanied by the formation of surface carbon, which hydrogenates to produce a methane peak at 442 K. A slight change was observed in the intensity of linear and bridged CO at a temperature around 442 K where the methane formation rate peaked. The small increase observed in linear CO could be ascribed to CO re-adsorption of CO and/or a slight change in the background at higher temperature. A rapid decrease was observed in the intensities of both linear and bridged CO which corresponds to the tailing methane shoulder in the range 494-593 K.

Comparison of peak temperatures and the amount of product desorbed for Ru/SiO_2 and $\text{Ru-Ag}/\text{SiO}_2$ catalysts is summarized in Table 2. Addition of silver to Ru/SiO_2 affects the absorbed state of bridged CO less than it does to linear CO. The intensity of bridged CO shows gradual decrease initially followed by rapid decrease in the range where the tailing methane peak was observed on Ru/SiO_2 catalysts. A rapid intensity decline of bridged CO species was accompanied with the formation of methane for $\text{Ag-Ru}/\text{SiO}_2$ at about the same temperature where the tailing methane peak was observed on Ru/SiO_2 . The significantly low wavenumber of bridged CO on $\text{Ru-Ag}/\text{SiO}_2$ compared to that of the bridged CO on Ru/SiO_2 appears to be due to the low concentration of bridged CO on $\text{Ru-Ag}/\text{SiO}_2$.

Addition of silver promotes the formation of gem-dicarbonyl, $\text{Ru}^+(\text{CO})_2$, as shown by the IR spectra for $\text{Ru-Ag}/\text{SiO}_2$ in Figure 4. Although the gem-dicarbonyl can be dissociated to surface carbon *via* the disproportionation reaction in the range 298-340 K during TPR, its role in CO dissociation over $\text{Ru-Ag}/\text{SiO}_2$ could be very limited under steady state reaction conditions (513-573 K). The reductive agglomeration of Ru^+ sites by CO and H_2 in the temperature range 513-573 K prevents the formation of gem-dicarbonyl and diminishes the Ru^+ sites.

The surface carbon species generated from linear and gem-dicarbonyl CO on $\text{Ru-Ag}/\text{SiO}_2$ during TPR where hydrogenated at temperatures higher than those from linear CO on Ru/SiO_2 , leading to a shift in the methane peak to a higher temperature. The results indicate that Ag favors hydrogen starving sites on the surface which result in the formation of higher hydrocarbons.

Linear CO is found to be more reactive than bridged CO

for methanation on Ru/SiO_2 consistent with the observation made by Mori *et al.* for Rh/SiO_2 .¹⁶ Only linear CO is reactive with H_2 for the formation of methane over Ru/SiO_2 via chemisorbed linear CO and tricarbonyl species. Under typical CO hydrogenation conditions at temperature around 473-573 K, bridged CO can be as important as linear CO because a significant extent of reaction of bridged CO occurs at these temperatures. The contribution of bridged CO site to methanation is also evidenced by the fact that a decrease in bridged CO site by the addition of Ag results in a decrease in steady-state methanation activity.

Conclusion

Combined IR and TPR-MS studies have shown that the silver produces bimetallic Ru-Ag sites that favor hydrogen deficient species on the surface. This results in the formation of CH_x hydrocarbons. The surface carbon is hydrogenated to methane with a maximum rate occurring at 442 K during TPR. The higher temperature for methane peak rate production on $\text{Ag-Ru}/\text{SiO}_2$ catalyst compared to Ru/SiO_2 catalyst is attributed to the presence of Ag-Ru bimetallic sites.

References

1. Wilson, T. P.; Kasai, P. H.; Ellgen, P. C. *J. Catal.* **1981**, *69*, 193.
2. Katzer, J. R.; Sleight, A. W.; Gajardo, P.; Michel, J. B.; Gleason, E. F.; McMillan, S. *Faraday Discuss. Chem. Soc.* **1991**, *72*, 282.
3. Watson, P. R.; Somorjai, G. A. *J. Catal.* **1981**, *74*, 282.
4. Worley, S. D.; Rice, C. A.; Mattson, G. A.; Curtis, C. W.; Guin, J. A.; Tarrer, A. R. *J. Chem. Phys.* **1982**, *76*, 20.
5. Yates, J. T.; Duncan, T. M.; Worley, S. D.; Vaughan, R. W. *J. Chem. Phys.* **1979**, *70*, 1219.
6. Solymosi, F.; Pasztor, M. *J. Phys. Chem.* **1986**, *90*, 5312.
7. Chaung, S. S. C.; Pien, S. I. *J. Catal.* **1992**, *138*, 536.
8. Underwood, R. P.; Bell, A. T. *J. Catal.* **1988**, *111*, 325.
9. Chaung, S. S. C.; Pien, S. I.; Narayanan, R. *Appl. Catal.* **1990**, *5*, 241.
10. Van den Berg, F. G. A.; Glezer, J. H. E.; Sachtler, W. M. H. *J. Catal.* **1985**, *93*, 340.
11. Chaung, S. S. C.; Goodwin, J. G., Jr.; Wender, I. *J. Catal.* **1985**, *95*, 435.
12. Bond, G. C.; Richards, D. G. *Appl. Catal.* **1986**, *28*, 303.
13. Kowalski, J.; Van der Lee, G.; Ponec, V. *Appl. Catal.* **1985**, *19*, 423.
14. Gysling, H. J.; Monnier, J. R.; Apai, G. *J. Catal.* **1987**, *103*, 407.
15. Ichikawa, M.; Fukushima, T. *J. Phys. Chem.* **1985**, *89*, 1564.
16. Mori, Y.; Mori, T.; Miyamoto, A.; Takahashi, N.; Hattori, N. T.; Murakami, Y. *J. Phys. Chem.* **1989**, *93*, 2039.
17. Mori, T.; Miyamoto, A.; Niizuma, H.; Takahashi, N.; Hattori, T.; Murakami, T. *J. Phys. Chem.* **1986**, *90*, 109.
18. Fujimoto, K.; Kameyama, M.; Kunugi, T. *J. Catal.* **1980**, *61*, 7.
19. Solymosi, F.; Tombacz, I.; Kocsis, M. *J. Catal.* **1982**, *75*, 78.
20. Koel, B. E.; Somorjai, G. A. In *Catalysis Sci. and Tech.*; Anderson, J. R., Boudart, M., Eds.; Springer-Verlag: Berlin, 1985; Vol. 7, p 159.
21. Tang, S. L.; Lee, M. B.; Yang, Q. Y.; Beckerle, S. T.; Ceyer, S. T. *J. Chem. Phys.* **1986**, *84*, 1876.
22. Solymosi, F.; Bansagi, T.; Novak, E. *J. Catal.* **1988**, *112*, 34.